



Erosion of ceramic coating applications under the influence of APS and HVOF methods

M. Demirci¹ · M. Bagci²

Received: 12 May 2021 / Accepted: 8 October 2022 / Published online: 2 November 2022
© King Abdulaziz City for Science and Technology 2022

Abstract

The erosion wear of the thermal barrier coating (TBC) application created by the ceramic topcoat effect on the substrate material and the high-temperature resistance has been researched in the study. Solid particle erosion effect has an important role in high-temperature applications such as energy conversion plants, gas turbines, and jet engine blades. In these applications where the ambient temperature varies and high-temperature effect is important, the deformation resistance is an important criterion in TBC's produced with atmospheric plasma spray (APS) and high-velocity oxy fuel (HVOF) methods as a result of the angular impact of the particles at certain velocities. In addition, its presence has an important impact in the adhesion effect between the substrate material and the ceramic top coating. In line with all these related criteria, the results of erosion wear in which the significance of the studies is gradually increasing will contribute to the fatigue failure of these coatings. To perform solid particle erosion experiments under high-temperature conditions (300 °C air temperature), experimental parameters were determined as three different erosive particle impact angles (30°, 60° and 90°) and fixed particle impact velocity (~50 m/s) with using constant particle size (200 μm Al₂O₃). As a result of the experiments, the erosion rates under the effect of temperature were determined depending on the angular and velocity variations of different coating methods. In the interpretation of the results, comments were made on the erosion rate variability using the effects of porosity, hardness, and surface roughness.

Keywords APS · Erosion resistance · High temperature · HVOF · Thermal barrier coating

Introduction

Thermal barrier coatings (TBCs) are protective coatings used in turbine blades to prevent materials exposed to high temperatures from being adversely affected by extreme temperatures. TBCs are especially used in the gas turbines intensively; it finds application in parts used as the aircraft engine, combustion chamber elements and power plants. Today, when the application area of gas turbines is expanding, the need for TBCs continues to increase.

TBCs generally consist of three layers; ceramic topcoat, bond coat and oxide layer which is formed over time by the penetrating oxygen and heat effect between these two layers (Kumar and Kandasubramanian 2016; Mehboob et al. 2020). The primary task of this oxide coating formed on the bond coating is to protect the substrate material from oxidation. The primary task of the ceramic top coating is to provide thermal insulation between the substrate material and the coating surface (Clarke et al. 2012). This type of coating, which was first used in the 1960s, started in the 1970s with the development of a two-layer TBC system by the National Aeronautics and Space Administration (NASA) Lewis Research Centre, and the TBC period that has been formed until today (Darolia 2013). As a result of using 6–8% of yttrium oxide weight in zirconia, TBCs with much better performance have been obtained by making the cubic phase in the top coating more stable (Stecura 1978; Miller 1997). In TBC coating method, atmospheric plasma spray (APS) and electron beam physical vapour deposition (EB-PVD) methods have been developed over time and have become

✉ M. Demirci
musa.demirci@karatay.edu.tr

¹ Faculty of Engineering and Natural Sciences, Department of Mechanical Engineering, KTO Karatay University, Konya, Turkey

² Faculty of Engineering and Natural Sciences, Department of Mechanical Engineering, Konya Technical University, Konya, Turkey

a commercial method for coating the TBC ceramic topcoat (Clarke 2018).

TBCs are complex systems that combine metallic and ceramic materials, developed to operate in extremely harsh thermal cycling conditions. The harmony between the metallic substrate and the ceramic top coating is achieved by the metallic bond coating. It is an important task of the bond coating to eliminate the incompatibility caused by the difference in thermal expansion coefficient of the ceramic top coating and substrate material by showing ductile material properties (Curry 2014). Today, alloys used in bond coating are denoted by the symbol MCrAlY (M=Ni, Co) and generally consist of NiCrAlY and NiCoCrAlY alloys (Meng et al. 2018; Song et al. 2008). The role of the elements used in the chemical composition of bond coatings is improving oxidation (Ni, Al), corrosion (Co) and adhesion properties (Y) of TBCs (Novak 1994; Birks et al. 2006). In bond coating; APS (atmospheric plasma spray), EB-PVD (electron beam physical vapour deposition) or HVOF (high-speed oxy fuel spray) methods are used (Chen et al. 2008). Bond coating can have different microstructure and thermal properties depending on the coating method used. It can be said that the compatibility of the bond coating with the ceramic top coating can determine the life of the TBC. This situation constituted the main motivation of this study. In this study, the adhesion properties of bond coatings which have the same ceramic top coating, but produced by different methods, have been tried to be determined by solid particle erosion wear experiments under high-temperature conditions.

Within the scope of this study, 8% yttria-stabilized zirconia (8YSZ) ceramic top coating by APS method was applied on NiCrAlY and NiCoCrAlY bond coatings produced by APS and HVOF methods. By examining the erosion wear of TBCs with different bond coatings and the same ceramic topcoat under the same conditions, the adhesion strength of bond coatings produced by different methods has been examined.

Experimental

The test samples were exposed to erosion wear at 30°, 60° and 90° erosive particle impact angle in a specially designed high-temperature solid particle erosion (HTSPE) test rig (Demirci and Bagci 2021). The experiments were carried out at temperatures of 21 °C and 300 °C. With the help of thermocouples in the test rig, it was ensured that the samples were tested under the same thermal conditions by measuring the temperature in the heating system and over the nozzle. Besides, the heating temperature of the sample was determined during the experiment with the help of a thermocouple attached to the back of the sample.

In the test rig, the erosive particle impact velocity can be adjusted between 10 m/s and 150 m/s. The double disc method was used in the measurement of the impact velocity (Ruff and Ives 1975) and erosion tests were carried out according to the distance between the nozzle and the sample measured with this method. In the double disc method, the time (t) required for a particle to pass through the distance (L) between two discs at an average velocity (ϑ) is expressed as L/ϑ from the linear motion equations. Based on the formula of arc length in a circle, the distance (S) between two tracks formed on the lower disc is found as specified in Eq. 1 where θ refers to the angle (radians) between the tracks, r refers to the trace radius (mm):

$$S = \theta \times r \quad (1)$$

Equation (1) becomes Eq. 2 when $\omega \times t$ is written instead of θ angle using rotational equations of motion:

$$S = (\omega \times t) \times r \quad (2)$$

In Eq. (2), instead of ω angular velocity (radian/s) expression, the definition depending on the motor rotation speed (n) is written and if L/ϑ is substituted for t time, an Eq. (3) is obtained according to the known parameters in measuring the particle velocity:

$$S = \left[\frac{2 \times \pi \times n}{60} \right] \times \frac{L}{\vartheta} \times r \quad (3)$$

When this equation is adjusted to determine the impact velocity, Eq. 4 expressing the erosive particle velocity results. 3D drawings of the discs used in the double disc method are shown in Fig. 1. The position of the produced discs in velocity measurement and the traces formed on the discs after the double disc method are given in Fig. 2:

$$\vartheta = \left[\frac{2 \times \pi \times n}{60} \right] \times \frac{L}{s} \times r \quad (4)$$

Samples

Inconel 718 was used as the substrate material in the test samples. Test samples were obtained in four groups. In the first group of samples, the bond coating consists of NiCrAlY (Amdry 962, Oerlikon Metco) powders obtained as a standard and these powders are coated on the surface with the APS method. Later, ceramic topcoat was made by APS method from 8YSZ (204 N, Oerlikon Metco) powder on this coating. Ceramic topcoat is applied in the same way in all sample groups. The second group of samples consists of NiCrAlY (Amdry 962, Oerlikon Metco) powders, which are obtained as a standard bond coating, and these powders are coated on the surface with the HVOF method to observe

Fig. 1 3D drawing of double disc method discs: **a** upper disc, **b** lower disc and **c** assembly side view (Demirci 2020)

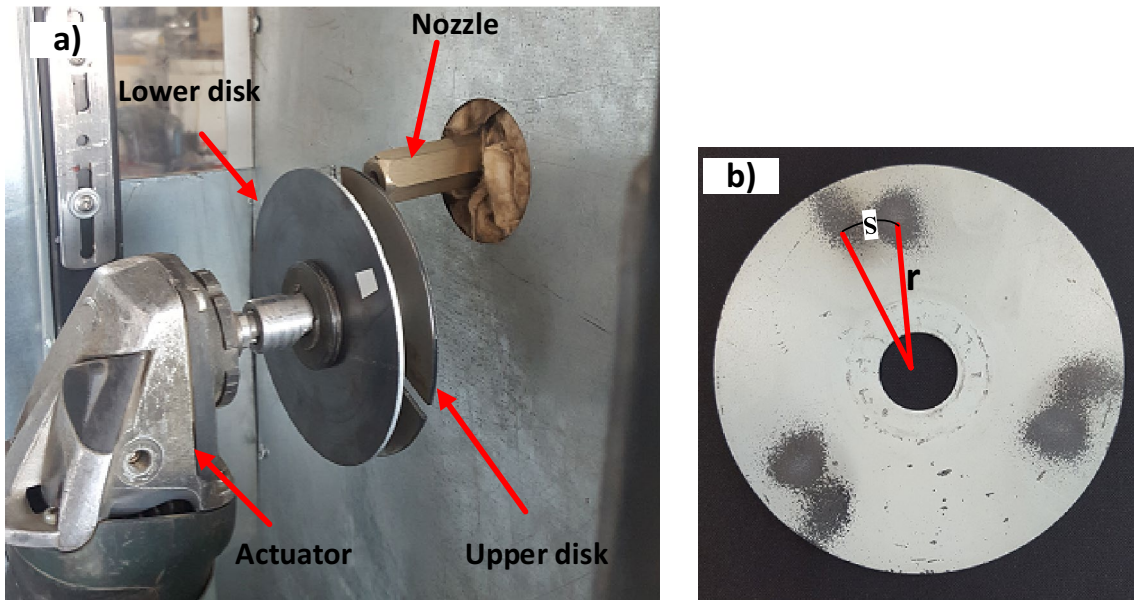
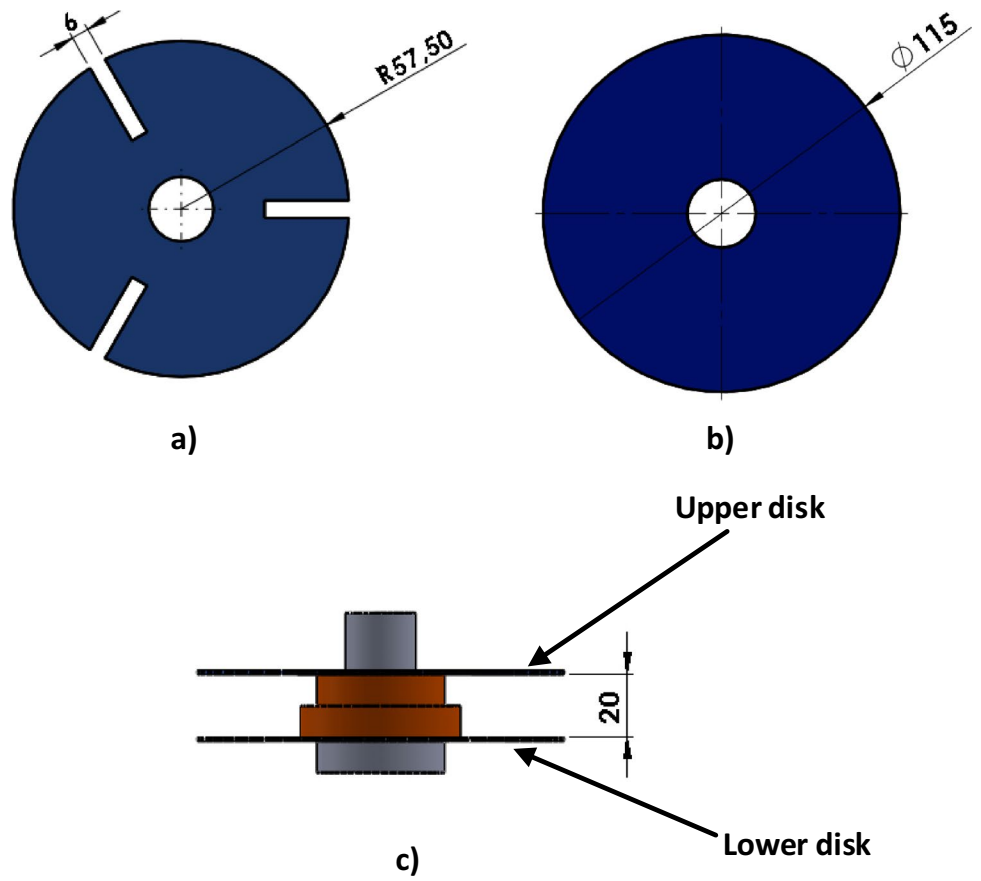


Fig. 2 Positioning of discs and formation of tracks: **a** driving the double disc by actuator, **b** the traces formed after wear on the lower disc (Demirci 2020)

the method difference. In the third group of samples, the bond coating consists of NiCoCrAlY (Amdry 365, Oerlikon Metco) powders were obtained as standard and these powders were coated on the surface by APS method. In the fourth sample group, NiCoCrAlY (Amdry 365, Oerlikon Metco) powders were used as bond coating powder, but it was coated on the surface with the HVOF method.

The porosity measurement of the samples was made with the “Mercury Porosimeter” (Micromeritics, USA). Mercury porosimeter is a widely used method in the literature to find the porosity diameter and distribution (Siebert et al. 1999; Vaßen et al. 2004; Curry et al. 2015). The working principle is based on the use of the high surface tension feature of the mercury, which does not react chemically with the surface of the material and does not wet the surface of the material (Mikijelj and Varela 1991). Since mercury does not spontaneously penetrate the pores by capillary action, it must be forced into the pores by applying external pressure. In this case, a pressure (P) must be applied so that the mercury can penetrate the pores, with the pores being accepted as cylindrical. This pressure is inversely proportional to the pore diameter (r) and is balanced by the surface tension (γ) of the mercury. This situation is expressed by the Washburn Eq. (5) (Diamond 2000):

$$P = \frac{-2\gamma\cos\theta}{r} \quad (5)$$

Here, θ refers to the contact angle between the material surface and mercury. Knowing the applied pressure and the material constants γ and θ values, the pore diameter (r) can be measured. Moreover, by knowing the volume of mercury penetrating the pore at each pressure change, the pore volume can be found depending on the pore diameter.

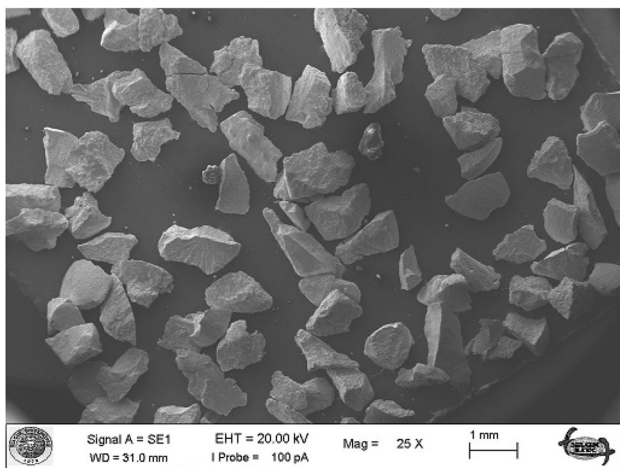


Fig. 3 SEM image of erosive particles (alumina)

Tests conditions

Solid particle erosion wear experiments were performed at two different temperatures (21 °C and 300 °C), three different angles (30°, 60° and 90°) and fixed impact velocity (50 m/s). In solid particle erosion tests, when high temperatures are reached, a corrosion or oxidation film begins to form on the material surface. This affects the erosion phenomenon. For this reason, a temperature of 300 °C, which will remain within the Regime 2 interval, where the erosion intensity will be high, was chosen as the experimental parameter (Birks et al. 2006). As erosive particles, non-spherical alumina (Al_2O_3) powders were used in 200 μm dimensions. These particles: due to its hardness, wear resistance and stability at high temperatures up to 2000 °C, it has been widely preferred by other researchers (Cernuschi et al. 2016; Schmitt et al. 2015; Wang et al. 2012, 2014) in the SPE wear experiments of materials with ceramic coating process. The SEM image and general properties of alumina powders used in SPE experiments are given in Fig. 3 and Table 1, respectively.

Solid particle erosion experiments can be carried out for samples of different sizes in the high-temperature solid particle erosion test rig. For this reason, the sample sizes were $20 \times 40 \times 2 \text{ mm}^3$. All experimental parameters are given in Table 2.

Results and discussion

The hardness, roughness and porosity measurement results of the test samples are given in Table 3. When we look at the hardness values of ceramic top coatings, since all surfaces are coated with the same material and the same method

Table 1 Properties of erosive particles (alumina)

Density (g/cm^3)	3,9 – 4,1
Hardness (Mohs)	9
Melting point ($^{\circ}\text{C}$)	2050

Table 2 High-temperature SPE test conditions

Test parameters	NiCrAlY/NiCoCrAlY (APS/HVOF)
Co composition (wt. %)	0/20
Erodent	Alumina (Al_2O_3)
Erodent size (μm)	≈ 200
Erodent shape	Angular
Impact angle, α ($^{\circ}$)	30–60–90
Impact velocity (m/s)	≈ 50
Test temperature ($^{\circ}\text{C}$)	21 and 300
Nozzle diameter (mm)	5
Air pressure (bar)	1

(APS), only small changes occurred in the hardness values due to the porosity that occurs during the coating process. Similarly, the roughness and porosity values of the ceramic top coatings were found to be close to each other. This can be interpreted as surfaces with similar mechanical properties show the same wear when subjected to solid particle erosion. However, since there are two coatings on the substrate and these coatings have different adhesion strengths between each other, the solid particle erosion test results differ. In this case, the study has revealed the difference in the adhesion strength between the coatings.

Impingement angle effect on the erosion rate

When the results of the erosion wear tests of ceramic top coated samples were examined in general, it was determined that the erosion rate increased due to the angle increase. This situation describes the erosion wear of brittle materials in the literature (Hutchings and Shipway 2017; Kleis and Kulu 2007). With this study, results compatible with the studies on ceramic top coatings in the literature have emerged (Cernuschi et al. 2016, 2011; Wang et al. 2012). In brittle materials, the most erosion wear occurs when the erosive particle impacts the surface at right angles (80°–90°). Since the material surface is ceramic and porous, erosive particles impacting at right angles facilitate crack propagation and, in this case, cause an increase in wear.

As a result of the experiments performed at room temperature depending on the impact angle, when Fig. 4 that gives the erosion rate is examined, the most erosion wear occurred in ceramic top coatings with cobalt-based bond coating (HVOF method). This situation showed that the same ceramic top coatings with similar mechanical properties exhibited different erosion rates under the same erosion test conditions due to different bond coating structures. Looking at the graph, the least erosion rate at 90° impingement angle where the most erosion wear occurs, again occurred in ceramic top coatings on which cobalt-based bond coating was applied. But the difference of these samples is that the bond coatings were coated with the APS method. Since the APS method creates a more porous structure than the HVOF method, the ceramic coating powders were better able to penetrate the surface space of the bond coatings coated with

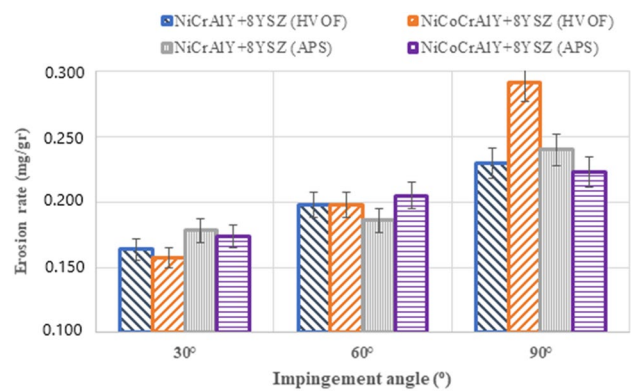


Fig. 4 Impact angle–erosion rate relationship of 8YSZ TBCs at 21 °C

the APS method and a higher strength adhesion occurred at the bond coating–ceramic top coating interface. Based on these results, it can be said that the coating method plays an important role in erosion resistance. Interestingly, the least erosion at 30° impact angle also occurred in samples with a cobalt-based bond coating. When the sample erosion rates occurring at the 30° impact angle and the sample erosion rates occurring at the 90° impact angle were compared, more differences were found in the 90° impact angle. In other words, the difference between the erosion rates of the test samples has increased as the test samples wear more. When the two (NiCrAlY + 8YSZ) TBC groups without cobalt-based bond coating are examined among themselves, it is seen that there is not much significant wear difference between them compared to whether the coating method is APS or HVOF. The samples with the bond coating produced by the HVOF method at an impact angle of 60° exhibited an almost similar wear condition. When we compare the coating methods according to the angle variability in general, we can conclude that the HVOF method is more sensitive to angle variability.

When we look at Fig. 5 in which the variation of the impact angle–erosion rate is given under high-temperature conditions (300 °C), again, the most erosion wear occurred in the test samples with cobalt-based bond coating and bond coating produced by HVOF method. Comparing the erosion rates at high temperature and room temperature at 90° impact angle, the samples generally exhibited less erosion rate at higher temperatures, albeit slightly. This situation

Table 3 Mechanical properties of test samples

	Average hardness (HR 15 N)	Average roughness value (Ra, μm)	Porosity (%)
NiCrAlY + 8YSZ (APS)	69.2 ± 1.99	10.5 ± 0.44	3.464
NiCoCrAlY + 8YSZ (APS)	73.8 ± 1.40	10.3 ± 0.6	3.831
NiCrAlY + 8YSZ (HVOF)	71.3 ± 2.15	11.1 ± 0.83	3.22
NiCoCrAlY + 8YSZ (HVOF)	72.4 ± 0.78	10.7 ± 0.1	3.55

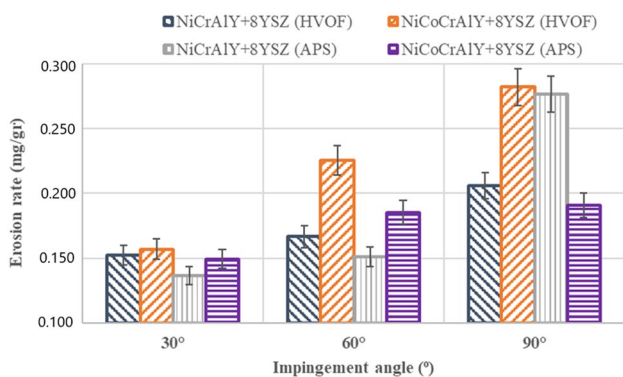


Fig. 5 Impact angle–erosion rate relationship of 8YSZ TBCs at 300 °C

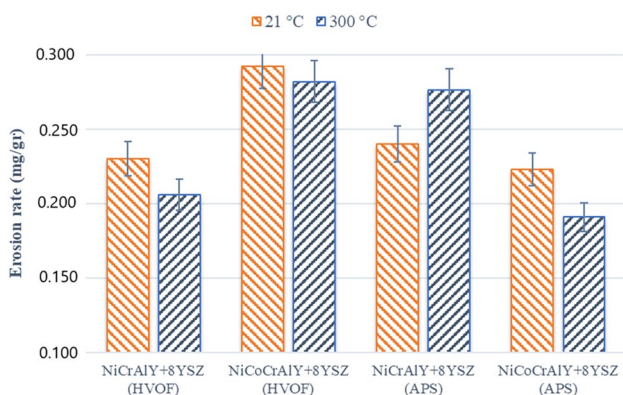


Fig. 6 Erosion rates change according to temperature variability at 90° impact angle

can be explained by the fact that the oxide layer formed on the surface with the increase of the temperature reaches a certain thickness and the impact velocity is low. As a result of the studies, it has been found that the oxide layer formed on the surface has a protective effect against erosive particles in the case that the erosive particle impact velocity is low in metals exposed to solid particle erosion at high temperatures (Birks et al. 2006). The decrease in erosion rate with temperature increase is explained in this way at low impact velocities. Similarly, when the erosion rates occurring at 300 °C were examined, the most angular change occurred in the test samples with bond coating coated with HVOF method. The most striking situation here is the increase in the erosion rate shown by the test samples with bond coating (NiCrAlY + 8YSZ) coated with APS method at right angles.

High-temperature effect on erosion rate

When Fig. 6, which compares the erosion rates exhibited by each experimental sample group at room temperature and at high temperatures, is examined, it is seen that the

temperature variation significantly changes the erosion rates. In addition, the temperature increases and decrease in erosion rates are clearly seen in three of the four test sample groups. Since only the bond coatings of the test samples with the same bond coating and ceramic top coating alloy are coated with a different method, the surface strength variability is clearly shown in the erosion rate graphs. When looking at this graph, an interpretation can be made as follows: it should be known which coating method exhibits better erosion resistance compared to the coating alloy. In addition, coating methods can be advantageous or disadvantageous in solid particle erosion wear depending on the alloy status. Wang, Liu, Mao, He and Feng (Wang et al. 2010) investigated the effect of temperature on solid particle erosion in the coatings used in steam turbines and as a result determined that the effect of temperature changes depending on the bond coating between the substrate and the top coating.

Conclusions

In this study, NiCrAlY and NiCoCrAlY bond coatings were deposited separately on the substrate material with different methods in order to produce TBC. 8% yttria-stabilized zirconia (8YSZ) ceramic top coating was applied on these bond coatings by APS method, resulting in the production of TBCs with different properties. The following results were obtained by performing erosion wear tests at different temperatures on these different TBCs produced.

1. NiCrAlY + 8YSZ and NiCoCrAlY + 8YSZ TBCs showed brittle material behaviour. The most erosion rate occurred at 90° impact angle.
2. TBCs with different bond coating forms but with the same ceramic topcoat composition showed different erosion rate changes at different temperature values under the same erosion test conditions. This situation revealed the importance of bond coatings in TBC materials.
3. NiCoCrAlY + 8YSZ TBCs with coated APS method performed more erosion resistance than HVOF method produced TBCs. The most erosion rate occurred at NiCoCrAlY + 8YSZ TBCs with coated HVOF method.
4. It was concluded that the particle impact variability creates more difference in the HVOF method due to the angular impact. In other words, the change in erosion resistance at 30° and 90° impact angles is less in coatings produced with the HVOF method compared to the APS method. This situation will cause to determine the preference priority for turbine components having aerodynamic form.

Declarations

Conflict of interest On behalf of all the authors, the corresponding author states that there is no conflict of interest.

References

- Birks N, Meier GH, Pettit FS (2006) Introduction to the high temperature oxidation of metals. Cambridge University Press, Cambridge
- Cernuschi F, Lorenzoni L, Capelli S, Guardamagna C, Karger M, Vaßen R, Von Niessen K, Markocsan N, Menuey J, Giolli C (2011) Solid particle erosion of thermal spray and physical vapour deposition thermal barrier coatings. *Wear* 271:2909–2918
- Cernuschi F, Guardamagna C, Capelli S, Lorenzoni L, Mack D, Moscatelli A (2016) Solid particle erosion of standard and advanced thermal barrier coatings. *Wear* 348:43–51
- Chen W, Wu X, Marple B, Nagy D, Patnaik P (2008) TGO growth behaviour in TBCs with APS and HVOF bond coats. *Surf Coat Technol* 202:2677–2683
- Clarke DR, Oechsner M, Padture NP (2012) Thermal-barrier coatings for more efficient gas-turbine engines. *MRS Bull* 37:891–898
- Clarke CR (2018) Thermal Barrier Coatings for Gas Turbines, Hong Kong University of Science and Technology
- Curry N (2014) Design of thermal barrier coating systems, University West
- Curry N, VanEvery K, Snyder T, Susnjari J, Bjorklund S (2015) Performance testing of suspension plasma sprayed thermal barrier coatings produced with varied suspension parameters. *Coatings* 5:338–356
- Darolia R (2013) Thermal barrier coatings technology: critical review, progress update, remaining challenges and prospects. *Int Mater Rev* 58:315–348
- Demirci M (2020) Investigation of solid particle erosion wear behaviour of thermal barrier coatings at high temperature, Mechanical Engineering, Konya Technical University, Graduate School of Education
- Demirci M, Bagci M (2021) Alternative system design for high temperature solid particle erosion wear problem. *Tribol Lett* 69:23
- Diamond S (2000) Mercury porosimetry: an inappropriate method for the measurement of pore size distributions in cement-based materials. *Cem Concr Res* 30:1517–1525
- Hutchings I, Shipway P (2017) Tribology: friction and wear of engineering materials, Butterworth-Heinemann
- Kleis I, Kulu P (2007) Solid particle erosion: occurrence, prediction and control, Springer Science & Business Media
- Kumar V, Kandasubramanian B (2016) Processing and design methodologies for advanced and novel thermal barrier coatings for engineering applications. *Particuology* 27:1–28
- Mehboob G, Liu M-J, Xu T, Hussain S, Mehboob G, Tahir A (2020) A review on failure mechanism of thermal barrier coatings and strategies to extend their lifetime. *Ceram Int* 46:8497–8521
- Meng G-H, Zhang B-Y, Liu H, Yang G-J, Xu T, Li C-X, Li C-J (2018) Vacuum heat treatment mechanisms promoting the adhesion strength of thermally sprayed metallic coatings. *Surf Coat Technol* 344:102–110
- Mikijelj B, Varela J (1991) Equivalence of surface areas determined by nitrogen adsorption and by mercury porosimetry. *Am Ceram Soc Bull* 70:829–831
- Miller RA (1997) Thermal barrier coatings for aircraft engines: history and directions. *J Therm Spray Technol* 6:35
- Novak R (1994) Coating development and use: case studies, Presentation to the Committee on Coatings for High-Temperature Structural Materials, National Materials Advisory Board, National Research Council, Irvine, California, 18–19
- Ruff A, Ives L (1975) Measurement of solid particle velocity in erosive wear. *Wear* 35:195–199
- Schmitt MP, Rai AK, Zhu D, Dorfman MR, Wolfe DE (2015) Thermal conductivity and erosion durability of composite two-phase air plasma sprayed thermal barrier coatings. *Surf Coat Technol* 279:44–52
- Siebert B, Funke C, Vaßen R, Stöver D (1999) Changes in porosity and Young's Modulus due to sintering of plasma sprayed thermal barrier coatings. *J Mater Process Technol* 92–93:217–223
- Song Y, Zhou C, Xu H (2008) Corrosion behavior of thermal barrier coatings exposed to NaCl plus water vapor at 1050° C. *Thin Solid Films* 516:5686–5689
- Stecura S (1978) Effects of compositional changes on the performance of a thermal barrier coating system. [yttria-stabilized zirconia coatings on gas turbine engine blades]
- Vaßen R, Traeger F, Stöver D (2004) Correlation between spraying conditions and microcrack density and their influence on thermal cycling life of thermal barrier coatings. *J Therm Spray Technol* 13:396–404
- Wang S-S, Liu G-W, Mao J-R, He Q-G, Feng Z-P (2010) Effects of coating thickness, test temperature, and coating hardness on the erosion resistance of steam turbine blades. *J Eng Gas Turbines Power* 132:022102
- Wang DS, Tian ZJ, Yang B, Shen LD (2012) Preparation and solid particle erosion behaviors of plasma-sprayed and laser-remelted ZrO₂-7wt.% Y₂O₃ thermal barrier coatings, applied mechanics and materials, *Trans Tech Publ* pp. 191–197
- Wang D, Tian Z, Shen L, Liu Z, Huang Y (2014) Effects of laser remelting on microstructure and solid particle erosion characteristics of ZrO₂-7wt.% Y₂O₃ thermal barrier coating prepared by plasma spraying. *Ceram Int* 40:8791–8799

Publisher's Note Springer Nature remains neutral with regard to jurisdictional claims in published maps and institutional affiliations.

Springer Nature or its licensor (e.g. a society or other partner) holds exclusive rights to this article under a publishing agreement with the author(s) or other rightsholder(s); author self-archiving of the accepted manuscript version of this article is solely governed by the terms of such publishing agreement and applicable law.